Biophysical Journal, Volume *121*

Supplemental information

Effects of vimentin on the migration, search efficiency, and mechanical resilience of dendritic cells

M. Reza Shaebani, Luiza Stankevicins, Doriane Vesperini, Marta Urbanska, Daniel A.D. Flormann, Emmanuel Terriac, Annica K.B. Gad, Fang Cheng, John E. Eriksson, and Franziska Lautenschläger

Supplementary Information to Effects of Vimentin on the Migration, Search Efficiency, and Mechanical Resilience of Dendritic Cells

M. Reza Shaebani, Luiza Stankevicins, Doriane Vesperini, Marta Urbanska, Daniel A. D. Flormann, Emmanuel Terriac, Annica K. B. Gad, Fang Cheng, John E. Eriksson, Franziska Lautenschläger

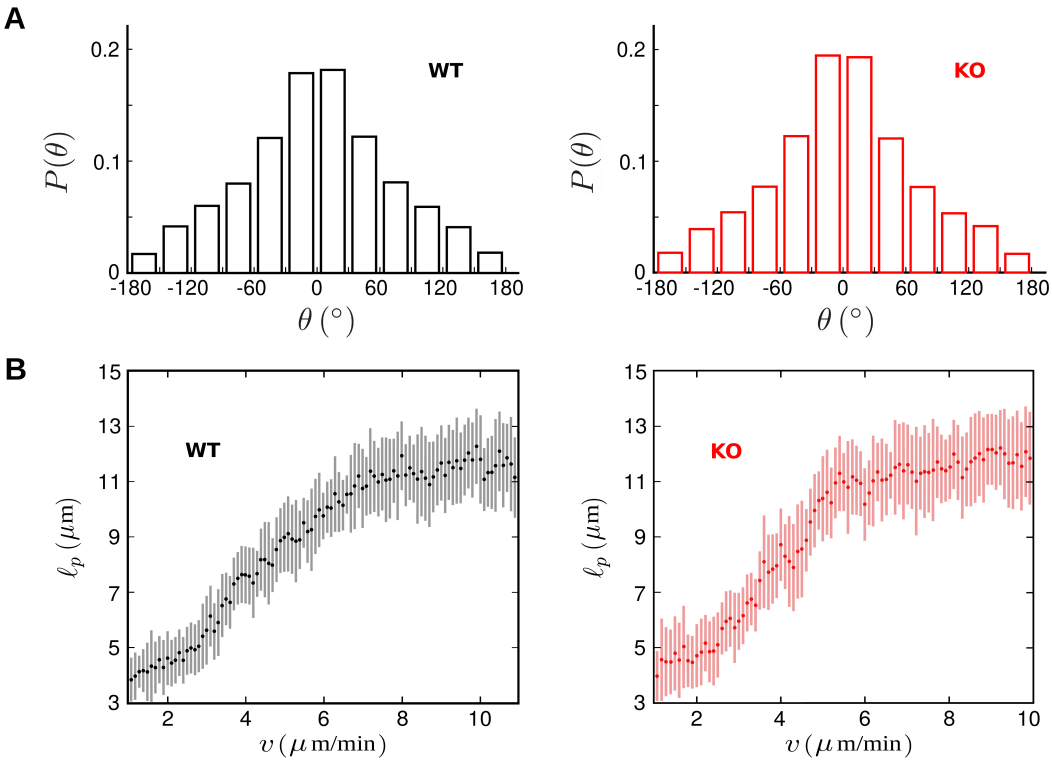

Figure S1: Comparison between the kinematics of bone-marrow-derived dendritic cells (BMDCs) with (WT) or without (KO) vimentin in two dimensions. (A) Probability distribution $P(\theta)$ of the turning angle θ at each recorded position of WT (left) and KO (right) BMDCs. (B) Local persistence length ℓ_p versus the migration speed v of WT and KO BMDCs. ℓ_p is deduced from $p = \cos(\theta) = e^{-\ell/\ell_p}$, with ℓ being the distance between two successive recorded positions [56]. The speed binning intervals of 0.1 μm/min are used.

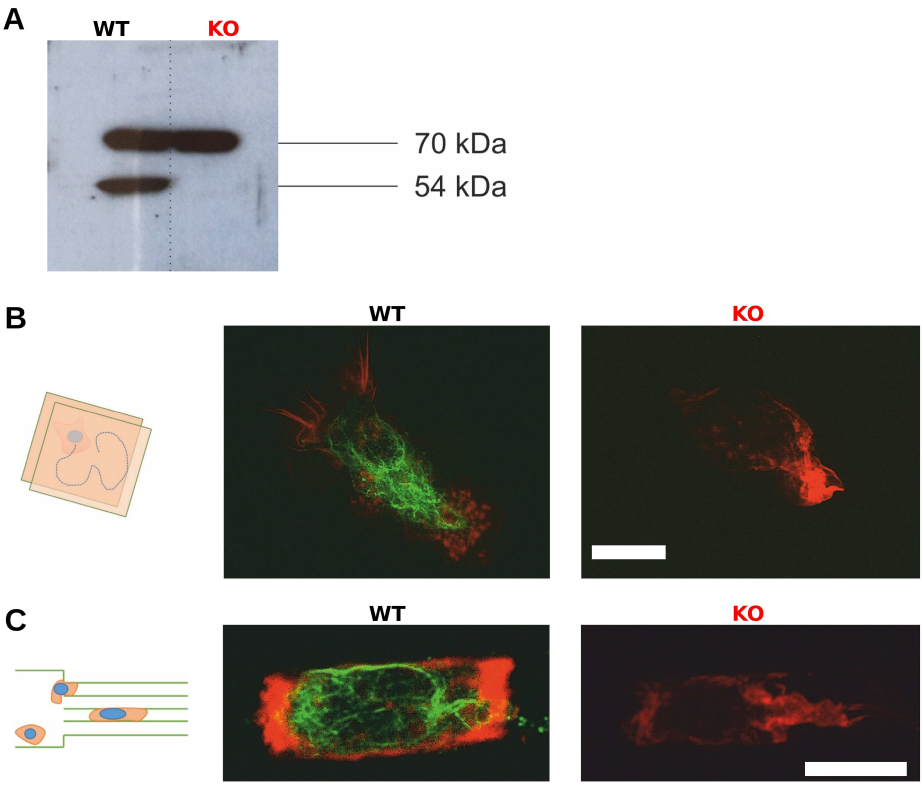

Figure S2: Cytoskeletal characterization in cells with (WT) or without (KO) vimentin. (A) Representative Western blot for protein quantification of vimentin in WT and KO primary BMDCs (54 kDa, vimentin), with loading control Hsc70 (70 kDa). (B,C) Representative images of WT and KO BMDCs for actin (red) and vimentin (green) filaments in 2D (B) and 1D (C) experiments. Scale bars, 10 μm.

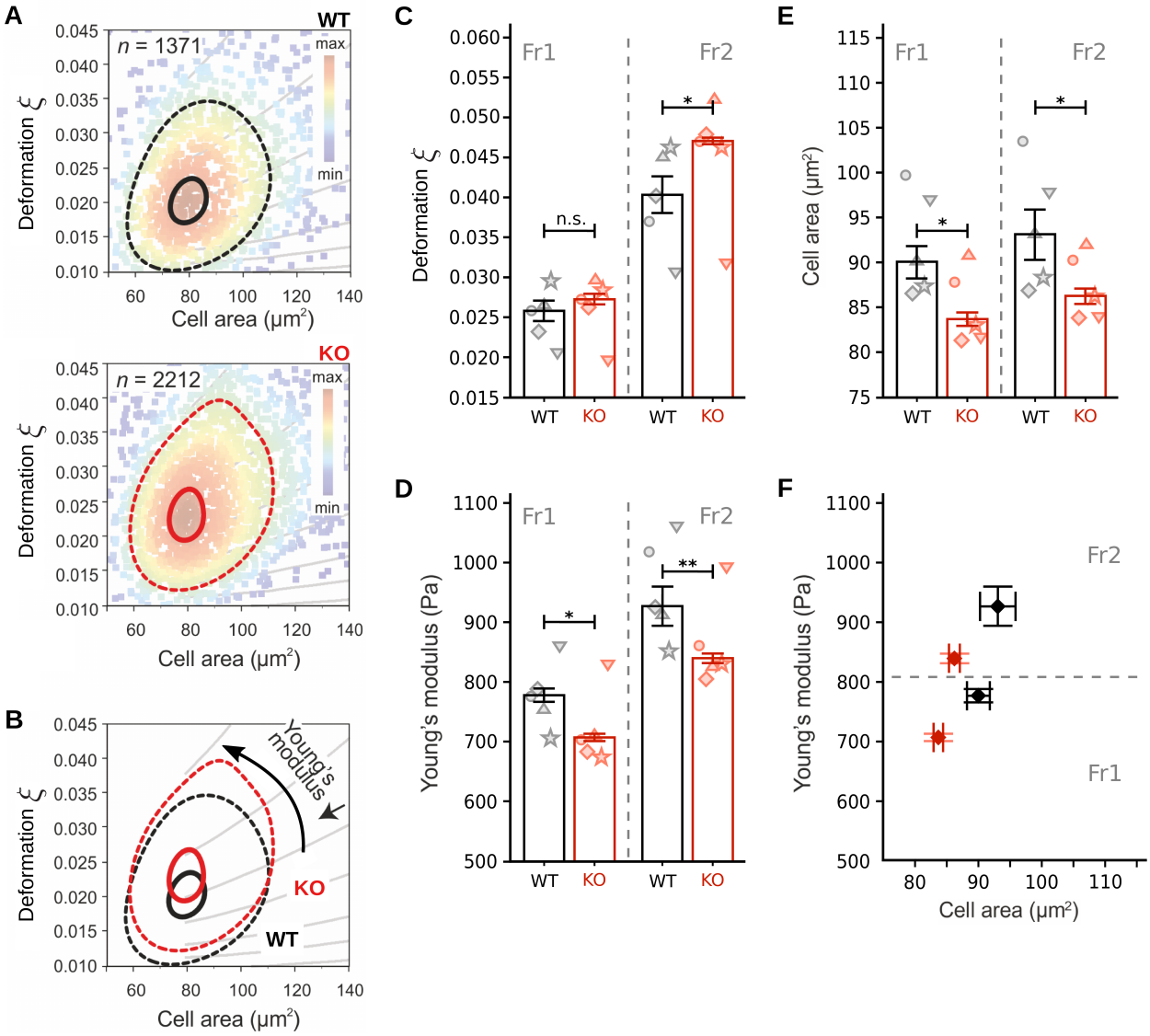

Figure S3: Real-time deformability cytometry analysis of global mechanical properties of BMDCs with (WT) or without (KO) vimentin. (A) Deformation-cell area scatter plots, showing a representative measurements of WT and KO BMDCs. The color map represents the event density and the contour plots delineate 50% density (dashed lines) and 95% density (solid lines). n is the number of measured cells. (B) Overlay of contours from (A). Grey lines are isoelastic regions from numerical simulations, which group cells of same mechanical properties. (C-E) Comparison of dimensionless deformation ξ (C), Young's modulus (D), and cell area (E) of WT and KO BMDCs, measured at two different flow rates: Fr1 ($0.16\,\mu$L.s^{-1}) and Fr2 ($0.32\,\mu$L.s^{-1}). The data represent median ± median absolute deviation. Circles denote the median values of five independent experiments. Statistical analysis is performed using linear mixed effects model. $*\,p<0.05$; $**\,p<0.01$; n.s., not significant. (F) Young's modulus versus cell area at two different flow rates.

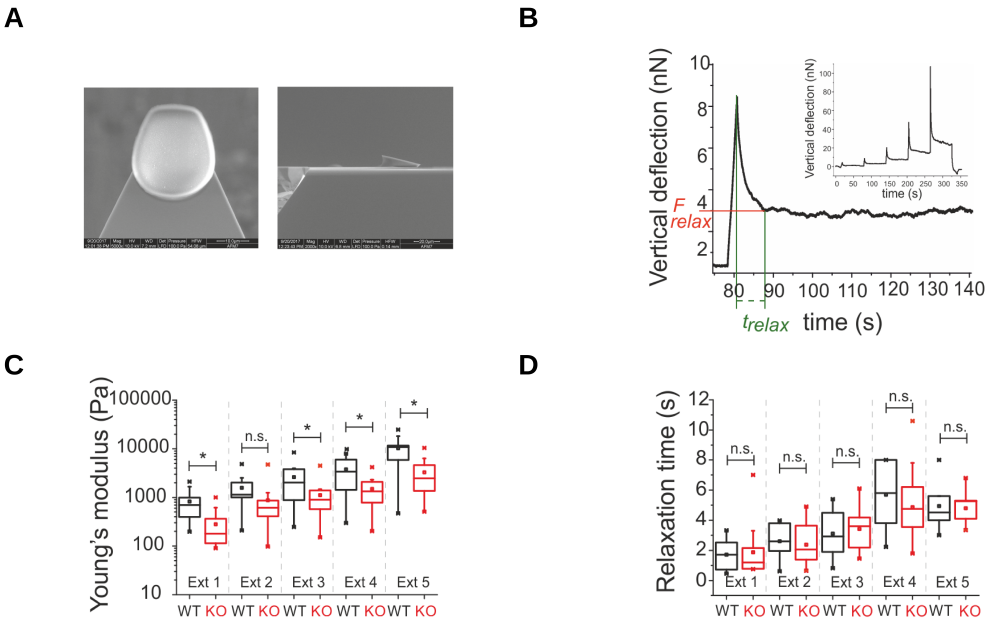

Figure S4: Force-mode atomic force microscopy analysis of dendritic cell mechanics. (A) Representative ventral and lateral electron microscopy images of wedged cantilevers used to evaluate the cell global mechanical response by atomic force microscopy. (B) Scheme of deformation graph used for analysis, showing measurement of relaxation time with atomic force microscopy. (C,D) Young's modulus (C) and relaxation time (D) of WT (black) and KO (red) BMDCs measured at different extents. Box plots for three independent experiments (total number of cells: 12 WT and 16 KO BMDCs) represent 25th to 75th percentile range with a line at the median and a square at the mean. Whiskers indicate extreme data points within 1.5× interquartile range (IQR). $*p<0.05$; n.s., not significant (t test).

Table S1. Comparison between the *in vitro* amoeboid migration of BMDCs with (WT) or without (KO) vimentin. The *apparent persistence* is a dimensionless quantity defined as the end-to-end distance divided by the actual length of the cell trajectory.

system	observable	cell type	mean ± standard error
1D	percentage of migrating cells	WT	72.2 ± 2.4 %
		KO	57.8 ± 5.3 %
	migration speed (μm.min^{-1})	WT	5.55 ± 0.09
		KO	4.98 ± 0.12
	apparent persistence	WT	0.680 ± 0.007
		KO	0.660 ± 0.010
2D	percentage of migrating cells	WT	52.7 ± 9.1 %
		KO	42.0 ± 10.1 %
	migration speed (μm.min^{-1})	WT	5.53 ± 0.05
		KO	4.53 ± 0.05
	path length (μm)	WT	383 ± 24
		KO	240 ± 19
	apparent persistence	WT	0.510 ± 0.004
		KO	0.510 ± 0.004
	local persistence	WT	0.44 ± 0.02
		KO	0.47 ± 0.02

Table S2. Mechanical properties of BMDCs with (WT) or without (KO) vimentin as analysed by real-time deformability cytometry. The experiments were repeated five times for each condition. The data in the right three columns represent median ± median absolute deviation.

flow rate (μL.s^{-1})	cell type	number of cells per experiment	total number of cells	dimensionless deformation ξ	Young's modulus (Pa)	cell area (μm^2)
0.16 [Fr1]	WT	3069	10238	0.0256 ± 0.0025	776 ± 22	90.1 ± 3.6
		2690				
		1371				
		1614				
		1494				
	KO	1929	9494	0.0271 ± 0.0012	706 ± 12	82.9 ± 1.2
		1991				
		2212				
		1836				
		1526				
0.32 [Fr2]	WT	1652	9093	0.0403 ± 0.0046	926 ± 66	93.1 ± 5.7
		2550				
		1055				
		1783				
		2053				
	KO	2134	10621	0.0469 ± 0.0008	838 ± 16	86.2 ± 1.8
		2218				
		2512				
		1971				
		1786				

Table S3. Mechanical properties of BMDCs with (WT) or without (KO) vimentin as analysed by atomic force microscopy. The mean value and the standard deviation of the relaxation time and the Young's modulus are shown.

extent	cell type	Young's modulus measurement		relaxation time measurement	
		number of cells	Young's modulus (Pa)	number of cells	relaxation time (s)
1	WT	12	826 ± 575	8	1.7 ± 1.1
	KO	16	280 ± 248	13	1.9 ± 1.8
2	WT	12	1573 ± 1221	7	2.6 ± 1.2
	KO	16	878 ± 1073	14	2.4 ± 1.3
3	WT	11	2617 ± 2295	8	3.1 ± 1.6
	KO	16	1118 ± 993	17	3.4 ± 1.5
4	WT	10	3782 ± 2731	7	5.7 ± 2.3
	KO	16	1491 ± 991	17	4.9 ± 2.4
5	WT	9	10275 ± 7669	6	4.9 ± 1.7
	KO	16	3288 ± 2583	17	4.8 ± 1.0